Distributed hydrostatic pressure measurement using phase-OTDR in a highly birefringent photonic crystal fibre

Sergei Mikhailov,[1,2] Li Zhang,[3] Thomas Geernaert[1,2], Francis Berghmans,[1,2] Kenny Hey Tow[3] and Luc Thévenaz[3]

[1] Vrije Universiteit Brussel, Department of Applied Physics and Photonics, Brussels Photonics (B-PHOT), Pleinlaan 2, B-1050 Brussels, Belgium
[2] Flanders Make, Oude Diestersebaan 133, 3920 Lommel, Belgium
[3] EPFL Swiss Federal Institute of Technology, Institute of Electrical Engineering, SCI-STI-LT, Station 11, CH-1015 Lausanne, Switzerland
Contact author e-mail: smikhail@b-phot.org

Abstract: We demonstrate a distributed hydrostatic pressure measurement based on phase-sensitive optical time-domain reflectometry in a highly birefringent photonic crystal fibre with a 0.4 bar pressure resolution and a 10 cm spatial resolution.

OCIS codes: (060.2370) Fiber optics sensors; (060.5295) Photonic crystal fibers; (120.4825) Optical time domain reflectometry; (260.1440) Birefringence; (290.5870) Scattering, Rayleigh.

1. Introduction

Distributed optical fibre sensing (DOFS) of axial strain and temperature [1, 2] is a well-established technology, which has found its place in the market, and which is also still the subject of extensive research and innovation efforts. However, there are almost no demonstrations of DOFS of hydrostatic pressure [3-5]. The main obstacle to such measurements is the small pressure sensitivity of standard step-index optical fibres [3, 6]. Dedicated fibres may provide a solution to this shortcoming. An internal structure of airholes, such as that used to obtain the so-called 'side-hole fibre', can increase the pressure sensitivity [7]. A hydrostatic load applied to the coating or cladding of such a fibre can induce a stress concentration in its core region, yielding a higher sensitivity to pressure. The birefringence of photonic crystal fibres (PCFs) can also be exploited for pressure sensing and can also be designed to feature an enhanced pressure sensitivity by optimizing the layout of the holey microstructure in the fibre's cross-section [8]. In addition, the birefringence also can be tailored to be negligibly sensitive to temperature. Such PCFs could therefore offer a low to negligible pressure measurement cross-sensitivity to temperature. In this report we exploit this potential and we discuss a distributed pressure measurement using a pressure-sensitive highly birefringent photonic crystal fibre and a phase-sensitive optical time-domain reflectometry (ϕOTDR) technique.

2. Working principle

Our approach is based on the detection of pressure-induced phase birefringence changes ΔB by means of ϕOTDR. This technique exploits Rayleigh backscattering along the fibre, caused by random density fluctuations in the fibre core, and compensates the local phase refractive index variations Δn with a frequency shift $\Delta\nu$ of the interrogating light pulse at a frequency ν [9].

2.1. Phase birefringence measurement

We measure the Rayleigh spectra $R_s(\nu, z_0)$ and $R_f(\nu, z_0)$ for both orthogonally polarized slow and fast optical axes of the fibre, at each position z_0. Because of the difference in refractive index of these two modes, the local spectra are shifted in frequency with respect to each other. Therefore, the cross-correlation function $C(\Delta\nu, z_0) = R_s(\nu, z_0)*R_f(\nu, z_0)$ (Fig.1) features a maximum at the frequency $\Delta\nu = \nu_s - \nu_f$, corresponding to the phase birefringence $B = n_s - n_f$ as given by:

$$\Delta\nu = \frac{\nu_s}{n_f^g} B \tag{1}$$

where n_f^g is the group refractive index along the fast axis.

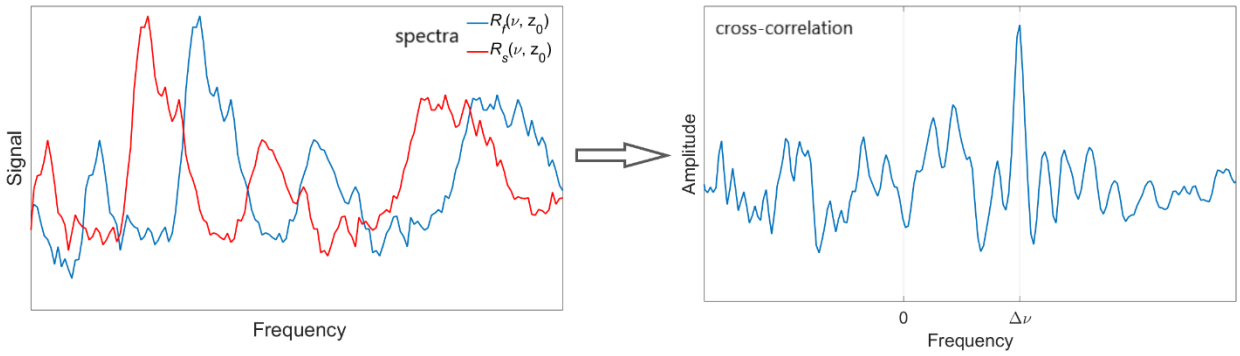

Fig.1. Working principle of a distributed birefringence measurement based on ϕOTDR traces along both orthogonally polarized modes of the birefringent fibre. The frequency shift between two local spectra leads to a cross-correlation peak at Δν.

2.2. Pressure measurement

We retrieve the pressure-induced birefringence change along the fibre using the spectral cross-correlations of ϕOTDR traces of a reference measurement at a pressure P_0 and measurements at different applied pressures P_i, i = 1, 2, for each of the orthogonal polarization axes. The cross-correlation functions $C_{s,f}(\Delta\nu, z_0, \Delta P_i) = R_{s,f}(\nu, z_0, P_0)^* R_{s,f}(\nu, z_0, P_i)$ are now maximal at the frequencies Δν, proportional to the equivalent pressure-induced changes of the refractive indices Δn_s and Δn_f along the slow and fast polarization axes (Fig. 2):

$$\Delta\nu_{s,f} = \frac{\nu_{s,f}}{n^g_{s,f}} \Delta n_{s,f}. \quad (2)$$

After obtaining the Δ*n* values for the fast and slow axes, we calculate the change of the phase birefringence as follows:

$$\Delta B = [\Delta n_s(P_2) - \Delta n_s(P_1)] - [\Delta n_f(P_2) - \Delta n_f(P_1)] \quad (3)$$

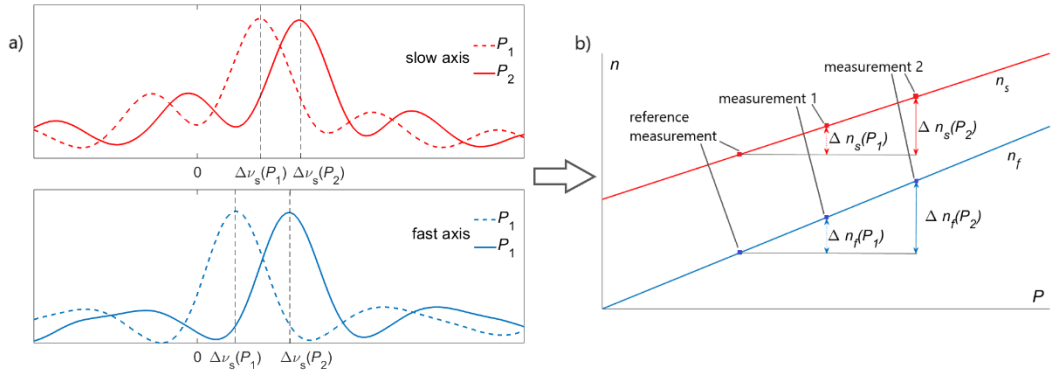

Fig.2. a) Frequency shifts Δν(*P*) obtained via cross-correlations of ϕOTDR signals of a reference measurement and measurements at different applied pressures converted into b) pressure-induced changes of refractive indices Δ*n*(*P*) in the slow and fast polarization axes as function of pressure.

The main drawback of this measurement is that it only provides the pressure-induced change of the birefringence Δ*B*, but not its absolute value *B*. The relation between Δ*B* and $\Delta P = P_2 - P_1$ is fibre dependent and is usually given by a simple linear relation.

3. Experimental setup

Figure 3 shows the scheme of the experimental ϕOTDR setup. We used a tuneable laser diode emitting at a wavelength around 1551 nm. We placed a polarization controller (PC) before the electro-optical modulators (EOM) to optimize the optical power. To form a 1 ns scanning pulse (yielding a 10 cm spatial resolution) with high extinction ratio, we used two EOMs driven by pulse generators, and we tuned the temperature of the laser to scan the pulse frequency. A polarizer (P) and polarization switch (PS) defined the orthogonal states of polarization of the interrogating pulse. An erbium-doped fibre amplifier (EDFA) amplified the signal, whilst a variable attenuator (VA) controlled the pulse power entering the fibre under test (FUT). We also used a second PC for aligning the pulse polarization along one of the polarization axes of the FUT. An EDFA amplified the Rayleigh backscattered signal, collected at port 3 of a

circulator, and then this signal was filtered using a tuneable optical filter (TOF) to reduce the amplified spontaneous emission (ASE) added by the EDFA. Finally, we monitored the backscattered signal with a 3-GHz bandwidth photodetector (PD) connected to a 10-GSps oscilloscope (Osc).

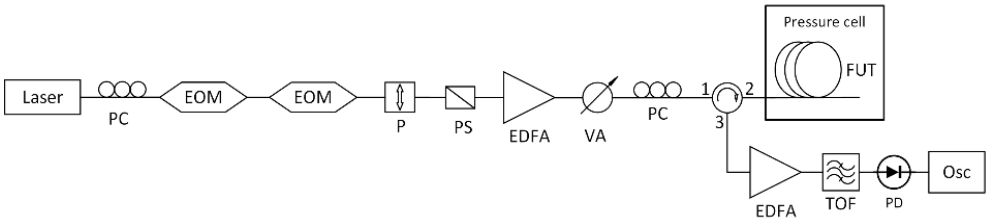

Fig.3. Scheme of the experimental ϕOTDR setup used for the distributed pressure measurement. Abbreviations are explained in the text.

4. Experimental results

4.1. Phase birefringence measurement

We carried out our measurements using a 4-m long highly birefringent (HiBi) "Butterfly" PCF [10], with a cross-section shown in Fig.4a. This PCF has a high polarimetric pressure sensitivity dB/dP (the simulated value of dB/dP is $-0.91\cdot10^{-6}$ bar^{-1}, as obtained with commercially available COMSOL Multiphysics® finite element modelling software, is), while the polarimetric temperature sensitivity dB/dT is almost zero. The low cross-sensitivity of the birefringence to pressure and temperature in this fibre makes it a good candidate for pressure sensing. Earlier measurements made with Brillouin optical time-domain analysis (BOTDA) have shown that the average phase modal birefringence is $7.83\cdot10^{-4}$ at the wavelength 1550 nm (corresponding to $\Delta\nu \approx 104$ GHz).

We tuned the frequency of the interrogating pulses, aligned to the slow and fast axes, to a difference of 104 GHz with respect to each other and we scanned it in a range of 60 GHz with 200 MHz steps. We calculated the cross-correlation of the ϕOTDR traces obtained from two consecutive measurements for orthogonal polarization axes along the fibre, with 10 cm spatial resolution, as shown in Fig. 4b. Based on the known frequency shifts, we obtained the corresponding birefringence distribution (Fig. 4c) using equation (1). A length of approximately 1 meter at the entrance of the fibre (not shown in the figures) was covered by a strong reflection occurring at the splice between the Panda-type lead-in fibre and the Butterfly PCF.

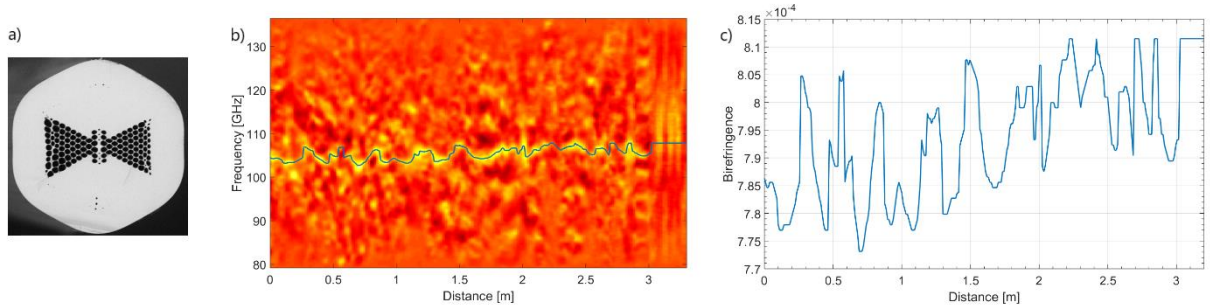

Fig.4. a) Cross-section of HiBi PCF. b) Cross-correlation of the ϕOTDR traces along slow and fast axis. c) Birefringence distribution along the fibre.

Fig.4c shows that the birefringence distribution in the PCF is non-uniform over its length, which is mainly attributed to small variations in the airhole microstructure along the fibre. The average birefringence $B = 7.91\cdot10^{-4}$ agrees well, however, with the value mentioned earlier.

4.2. Pressure measurement

To measure the pressure sensitivity of the FUT, we placed it in a pressure chamber, and we applied pressures of 0, 1 and 2 bar relative to atmospheric pressure. We scanned the pulse frequency in a 40 GHz range with 60 MHz steps and we computed the spectral cross-correlations of the Rayleigh traces at each pressure value. Fig.5a and Fig.5b show the pressure-induced frequency shifts and corresponding ΔB, as calculated using equations (2) and (3).

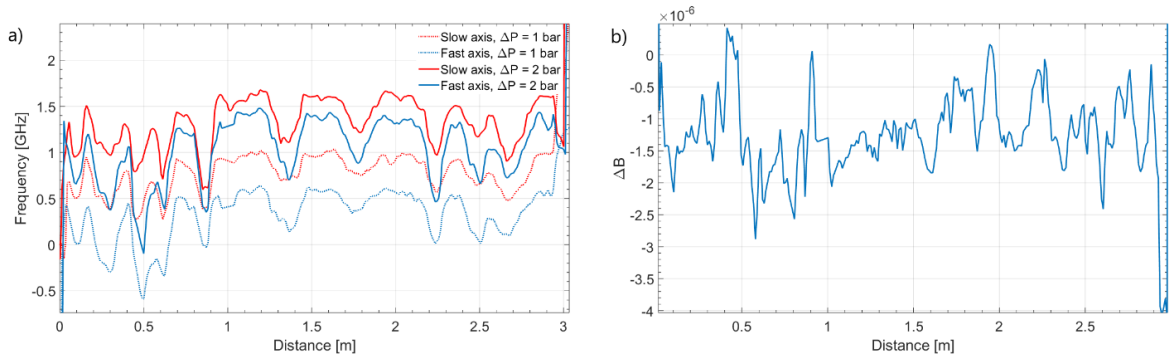

Fig.5. a) Pressure-induced frequency shift of the Rayleigh traces along the slow and fast axes. b) Birefringence change induced by pressure change of 1 bar.

Fig.5b shows that the response of the PCF is considerably non-uniform over its length. The mean pressure sensitivity of the birefringence is $dB/dP = -(1.21\pm0.4)\cdot10^{-6}$ bar^{-1} (corresponding to $d\nu/dP = -150$ MHz/bar). This value is in reasonable agreement with the simulations results. The pressure sensitivity is significantly larger than in other proposed distributed pressure measurements [3-5] with PCFs, and allows for sub-bar measurement resolution (0.4 bar for a frequency scanning resolution of 60 MHz). The pressure resolution can be further improved by implementing a finer pulse frequency tuning. Resolving smaller ΔP also calls for improving the uniformity of the birefringence along the fibre. The main limitation of the measurements, based on the detection of ΔB, stems from the fast longitudinal fluctuations (shorter than the spatial resolution) of the birefringence, leading to broadening and amplitude reduction of the correlation peak. This issue can be potentially resolved by using a better spatial resolution, but at the expense of spectral broadening of the correlation peak, which in its turn complicates the detection of small ΔB.

5. Conclusion

We demonstrated distributed hydrostatic pressure sensing based on ϕOTDR in a HiBi PCF with an average pressure sensitivity of -150 MHz/bar at a spatial resolution of 10 cm and a pressure measurement resolution of 0.4 bar.

6. Acknowledgements

This work was performed in the framework of ITN-FINESSE, funded by the European Union's Horizon 2020 research and innovation program under the Marie Sklodowska-Curie Action grant agreement n° 722509. The authors would like to acknowledge financial support from Vrije Universiteit Brussel's Methusalem and Hercules Foundations, as well as the Belgian Science Policy Interuniversity Attraction Pole P7/35.

7. References

[1] T. Horiguchi, K. Shimizu, T. Kurashima, M. Tateda, and Y. Koyamada, "Development of a distributed sensing technique using Brillouin scattering," J. Lightwave Technol. **13**(7), 1296–1302 (1995).

[2] Y. Koyamada, M. Imahama, K. Kubota, and K. Hogari, "Fiber-optic distributed strain and temperature sensing with very high measurand resolution over long range using coherent OTDR," J. Lightwave Technol. 27(9), 1142–1146 (2009).

[3] Y. H. Kim, H. Kwon, J. Kim, and K. Y. Song, "Distributed measurement of hydrostatic pressure based on Brillouin dynamic grating in polarization maintaining fibers," Opt. Express 24(19), 21399–21406 (2016).

[4] T. Chen, Q.Wang, R. Chen, B. Zhang, C. Jewart, K. P. Chen, M. Maklad, and P. R. Swinehart, "Distributed high-temperature pressure sensing using air-hole microstructural fibers," Opt. Lett. 37(6), 1064-1066 (2012).

[5] L. Teng, H. Zhang, Y. Dong, D. Zhou, T. Jiang, W. Gao, Z. Lu, L. Chen, and X. Bao, "Temperature-compensated distributed hydrostatic pressure sensor with a thin-diameter polarization-maintaining photonic crystal fiber based on Brillouin dynamic gratings," Opt. Lett. 41(18), 4413-4416 (2016).

[6] S. Le Floch, and P. Cambon. "Study of Brillouin gain spectrum in standard single-mode optical fiber at low temperatures (1.4–370 K) and high hydrostatic pressures (1–250 bars)." Optics communications 219(1-6), 395-410 (2003).

[7] H. M. Xie, P. Dabkiewicz, R. Ulrich, and K. Okamoto, "Side-hole fiber for fiber-optic pressure sensing," Opt. Lett. 11(5), 333-335 (1986).

[8] M. Szpulak, T. Martynkien, and W. Urbanczyk, "Effects of hydrostatic pressure on phase and group modal birefringence in microstructured holey fibers," Appl. Opt. 43(24), 4739-4744 (2004)

[9] M. A. Soto, X. Lu, H. F. Martins, M. Gonzalez-Herraez, and L. Thévenaz, "Distributed phase birefringence measurements based on polarization correlation in phase-sensitive optical time-domain reflectometers," Opt. Express 23(19), 24923-24936 (2015).

[10] T. Martynkien, G. Statkiewicz-Barabach, J. Olszewski, J. Wojcik, P. Mergo, T. Geernaert, C. Sonnenfeld, A. Anuszkiewicz, M. K. Szczurowski, K. Tarnowski, M. Makara, K. Skorupski, J. Klimek, K. Poturaj, W. Urbanczyk, T. Nasilowski, F. Berghmans, and H. Thienpont, "Highly birefringent microstructured fibers with enhanced sensitivity to hydrostatic pressure," Opt. Express 18(14), 15113-15121 (2010).